Optical Properties of Glycated and Non-Glycated Hemoglobin – Raman/Fluorescence Spectroscopy and Refractometry

Ekaterina N. Lazareva[1,2*], Andrey Y. Zyubin[3], Natalya I. Dikht[4], Alla B. Bucharskaya[1,2,4], Ilya G. Samusev[3], Vasily A. Slezhkin[3,5], Vyacheslav I. Kochubey[1,2], and Valery V. Tuchin[1,2,6]

[1] Science Medical Center, Saratov State University, 83 Astrakhanskaya str., Saratov 410012, Russia

[2] Laboratory of Laser Molecular Imaging and Machine Learning, Tomsk State University, 36 Lenin av., Tomsk 634050, Russia

[3] REC "Fundamental and Applied Photonics. Nanophotonics", Immanuel Kant Baltic Federal University, 14A Nevskogo str., Kaliningrad 236041, Russia

[4] Saratov State Medical University named after V. I. Razumovsky, 112 Bolshaya Kazachia str., Saratov 410012, Russia

[5] Department of Chemistry, Kaliningrad State Technical University, 1 Sovietsky prospect, Kaliningrad 236022, Russia

[6] Laboratory of Laser Diagnostics of Technical and Living Systems, Institute of Precision Mechanics and Control, FRC "Saratov Research Centre of the Russian Academy of Sciences", 24 Rabochaya str., Saratov 410028, Russia

*** e-mail:** LazarevaEN@list.ru

Abstract. In this study, the optical properties of glycated (HbA1c) and non-glycated (Hb) hemoglobin are compared using Surface-enhanced Raman spectroscopy (SERS), spectrofluorimetry, and refractometry. Analysis of the spectral shift of SERS spectra showed good discrimination between two hemoglobins indicating differences in their molecular structure. The fluorescence spectra measured at excitation wavelengths of 260, 270, and 280 nm also indicate differences in the molecular structure of these hemoglobins. For the first time refractive index temperature increments were measured for HbA1c in a wide wavelength range in the visible and NIR as $-(1.35 \pm 0.11) \times 10^{-4}\,°C^{-1}$ and compared with normal hemoglobin ($dn/dT = -(1.02 \pm 0.12) \times 10^{-4}\,°C^{-1}$). The comparison of temperature RI increments for hemoglobin obtained from the whole blood of healthy volunteers and diabetic patients is also done. The data obtained can serve as a basis for further study of the optical properties of glycated hemoglobin and other glycated proteins. © 2022 Journal of Biomedical Photonics & Engineering.

Keywords: refraction; refractive index; temperature increment; fluorescence; Raman spectroscopy; SERS; hemoglobin; glycated hemoglobin HbA1c.

Paper #3479 received 28 Feb 2022; revised manuscript received 25 Apr 2022; accepted for publication 25 Apr 2022; published online 14 May 2022. doi: 10.18287/JBPE22.08.020303.

1 Introduction

According to current statistical data, the incidence of diabetes mellitus is increasing every year. Among methods of diagnostics are methods based on the quantitative determination of glycated proteins, which are biological markers of the disease [1–3]. One of them that is often used as a marker is HbA1c which is formed by the nonenzymatic glycation of hemoglobin exposed to free blood glucose and therefore has a strong correlation with the average glucose concentration in the bloodstream in the preceding three-month period (life span of the erythrocytes). Because of this strong correlation, HbA1c levels have been regularly used to monitor long-term glucose control in established diabetics and have been recently approved for screening for diabetes ($HbA1c \geq 6.5\%$) and prediabetes ($5.7\% \leq HbA1c \leq 6.4\%$) [1–6].

Currently, there are more than 20 methods for the determination of glycated hemoglobin, such as cation exchange chromatography, electrophoresis, affinity chromatography, and immunoassay, but each of them measures various fractions of glycated hemoglobin [1–3]. Most of the methods used are based on the chemical separation of the non-glycated and glycated hemoglobin fractions and the subsequent determination of the concentration of glycated hemoglobin by subtracting the unbound form from the total amount of hemoglobin. These methods are invasive and have significant drawbacks, for example, chromatography is very sensitive to changes in temperature and pH [2].

At present, optical methods represent ample opportunities and are promising for the development of rapid and non-invasive methods of diagnosis and therapy of early stages of diseases such as diabetes, cancer, and others [7–11]. Knowledge of the optical properties of blood, hemoglobin, glycated hemoglobin, and its distinctive features will help in developing a quick, simple, and noninvasive method for diagnosing these diseases. For example, *in vivo* flow cytometry of diabetic patients with melanoma may have additional background signals from glycated erythrocytes [7].

In this paper, a comparative analysis of the optical properties of glycated and normal hemoglobin was performed by using refractometry, spectrofluorimetry and Surface-enhanced Raman spectroscopy (SERS). Optical methods chosen in this study are most often used as diagnostic techniques and allow for detection of substances by differences in their molecular structure [12–14]. Raman spectroscopy (RS) is widely used as a powerful diagnostic tool in biomedical research due to the possibility to provide fingerprint information of the molecular composition and structure of a sample, such as proteins, lipids, etc. [15]. For diabetes diagnosis, Han et al. [16] used RS to analyze the serum of diabetic patients as Barman et al. [17] used it to detect the glycated hemoglobin in hemolysate model formed by two-component mixture (Hb and HbA1c) [16, 17]. As an alternate method for HbA1c detection, Ishikawa and co-workers have recently reported the application of Surface-enhanced resonance Raman spectroscopy (SERRS) [18]. Although promising in approach, precise quantification of the analyte of interest (HbA1c) using SERRS is difficult (as also was noted by the authors), because of poor spectral reproducibility and the generation of spurious background signals [19]. The use of RS allows for a qualitative analysis of the samples and clarifies the results obtained by refractometric and fluorescent methods. It has been shown the possibility of SERRS to identify the distinctive features of glycated forms of proteins (albumin, hemoglobin) from non-glycated [14, 20, 21]. Native fluorescence spectroscopy of blood plasma in rats with experimental diabetes was used to identify the characteristic features of the fluorescence spectrum associated with glucose metabolism. The incubation of albumin with glucose *in vitro* showed that there is a new fluorescence band, which is caused by the formation of cross-links giving fluorescence in the range 400–430 nm upon excitation at 320–350 nm. The fluorescent properties of this band are similar for different proteins (for example, for albumin and collagen), since one of the main glycation products that causes this fluorescence is pentosidine [14]. The refractive index (RI) is one of the most important optical characteristics of tissues and the knowledge of its dispersion and temperature dependences for various forms of hemoglobin is important for understanding the changes in the optical properties of blood and biological tissues [13, 22–25] Since the structure and composition of tissues and correspondingly their optical properties are changing in the course of pathology development, then several research groups have suggested the RI as a marker for differentiation of normal and pathological tissue, including experimental diabetes in animals [13, 22, 23].

In these studies, a comparative fluorescence analysis of hemoglobins was done for excitation wavelengths of 260, 270 and 280 nm. We also applied SERS to detect spectra from the dried drops of Hb and HbA1c. The RIs of two forms of hemoglobin were measured for 12 visible and NIR wavelengths (480–1550 nm) at temperature 25 °C and for wavelengths 546, 589, 644, 930 nm at temperatures from 23 to 43 °C. The RIs of hemoglobin solution for the control and diabetic groups were measured for a temperature range from 25 to 50 °C at 12 wavelengths.

2 Methods and Materials

The optical properties of solutions of glycated and non-glycated forms of hemoglobin were investigated by using a multimodal approach with three independent optical methods, which allows us to make a detailed comparison of optical properties and to reveal specific features of hemoglobins for their discrimination.

2.1 Samples

As samples of the study, solutions of pure Hb and HbA1c were taken. Lyophilized powder of human Hemoglobin (Hb) and hemolysate of glycated hemoglobin (HbA1c) (Sigma-Aldrich) were used. The dilution was performed with a physiological solution of 0.9% NaCl.

Refractometric measurements were also performed for hemoglobin obtained from the whole blood of healthy volunteers (control group) and patients with diabetes mellitus (diabetes group). Whole blood was drawn from the human vein. Immediately after collecting blood into a test tube, heparin was added to it. The sample of blood was taken at the State Health Care Organization “Saratov City Clinical Hospital No. 2 named after V. I. Razumovsky with the permission of the volunteers (patient information consent). The level of glucose in the blood samples was 14.5, 11.7, and 8.8 mmol/l according to the results of the biochemical analysis. To separate blood into fractions, centrifugation for 10 min at 2000 rpm and at room temperature was provided. This

resulted in the separation of blood plasma, leuko-platelet layer, and RBC suspension. To conduct hemolysis and preparation of hemoglobin solutions, RBC suspension was separated and placed in a vial for freezing in a freezer at a temperature of −15 °C for 24 h.

2.2 SERS Experiments

SERS spectra were obtained by CENTAUR U HR (NanoScanTechnology LTD, Russia and ZAO SolarLS, Republic of Belarus) unit equipped with a He-Ne laser (Coherent Inc., USA) with excitation ($\lambda = 632$ nm, radiation power of 37 mW on the sample with the spot of 3.2 μm in diameter). SERS spectra were recorded using a thermoelectrically cooled CCD with a temperature of –40 °C and 5 sec acquisition time set for detector matrix. A spectrometer with a holographic diffraction grating of 600 grates/mm was used. Wavenumber reproduction accuracy was 1 cm^{-1}. The spectral resolution was 1 cm^{-1}. Rayleigh scattering has been eliminated by the use of a notch filter. The CENTAUR U scientific has been calibrated with silicon at a static spectrum centered at 520 cm^{-1}. The sample holder has been mounted on a standard stage for an Olympus BX41 microscope. For SERS, substrates of island anodically-dissolved silver, deposited electrochemically on a polished copper base with an anodic dissolution depth of silver of 500 nm, were used. Solutions of hemoglobin and glycated hemoglobin at a concentration of 3 g/l each were deposited as drops on the substrate. Samples were dried in the open air. As a result, a ring with a higher thickness of the sample was formed at the edges of the dried drops. The diameter of the rings was not more than 3 mm. Measurements were carried out for 5 samples of each solution. KnowItAll Vibrational Spectroscopy Edition (Willey, UK) software was used for linear baseline correction and normalization of all original spectra and further analysis of peaks position and its intensity.

2.3 Fluorescence Spectroscopy

The studies were carried out using a fluorescence spectrometer Cary Eclipse (Varian, Belgium). Excitation wavelengths were selected as 260, 270, and 280 nm. The solutions for measurements were highly diluted to a concentration at which the optical density is 0.1 in the spectral region of excitation. The optical density was measured on a spectrometer UV-3600 (Shimadzu, Japan). The spectra of fluorescence excitation were processed by a Gaussian analysis in the program OriginLab Pro (USA).

2.4 Refractometric Measurement

The commercial Multi-wavelength refractometer Abbe DR-M2/1550 (Atago, Japan) was used to measure the RI of solutions of Hb and HbA1c at a concentration of 3 g/l each and hemoglobin solution from healthy donors and patients with diabetes mellitus. In the setup, the source of radiation was a high-power candescent lamp. To select the wavelength, we used narrow-band interference filters for (480 ± 2), (486 ± 2), (546 ± 2), (589 ± 2), (644 ± 2), (656 ± 2), (680 ± 5), (800 ± 5), (930 ± 6), (1100 ± 26), (1300 ± 25), and (1500 ± 25) nm. The measurement error introduced by the instrument amounts to ±0.0002. At the beginning of every measurement, the calibration of the instrument using the known tabulated value of the RI of distilled water was executed. The sample temperature during the measurements was kept by water circulation in the refractometer provided by a thermostat. The temperature was 25 °C when measuring the RI for 12 wavelengths. The RI of Hb and HbA1c was measured at the wavelengths of 546, 589, and 644 nm at temperatures from 23 °C to 43 °C. The RI of hemoglobin for the control and diabetic groups was measured for a temperature range of 25 °C to 50 °C at 12 wavelengths. The RI was calculated as averaged over 3 measurements for each of 3 samples of Hb, HbA1c, hemoglobin from the whole blood of a healthy donor and of a patient with diabetes mellitus.

3 Results and Discussion

SERS spectra of Hb and HbA1c are shown in Figs. 1, 2. Determination of the position of the peaks and normalization procedure were carried out using KnowItAll Vibrational Spectroscopy Edition (Willey, UK) software. First derivative for both Hb and HbA1c were taken to indicate difference in the spectral intensity.

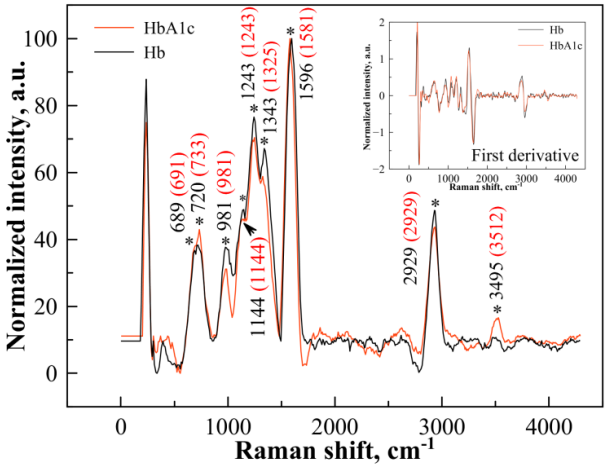

Fig. 1 Normalized SERS spectra acquired from dry drops of Hb (black line) and HbA1c (red line). Full spectral range (includes the first derivative of the spectra in the right top corner).

Differences in the spectra for Hb and HbA1c are observed mainly in the "fingerprint" region 0–1800 cm^{-1}. In this region, the position of the maxima of 10 peaks is established, the position of all peaks and their intensity have been described and analyzed to detect differences in the structure. The Hb and HbA1c spectra have been differentiated primarily based on peak shifts and secondary – on intensity.

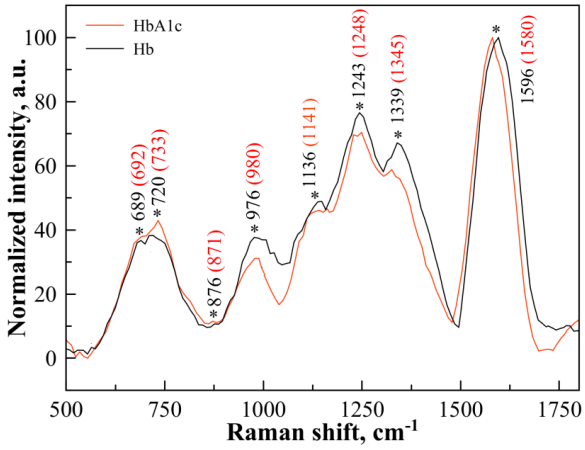

Fig. 2 Normalized SERS spectra acquired from dry drops of Hb (black line) and HbA1c (red line) for 500–1800 cm^{-1} "fingerprint" region.

Fig. 2 displays normalized SERS spectra of Hb and HbA1c. The band of FeO_2 at 1136 cm^{-1} [38] was observed for Hb and very low and shifted for HbA1c, confirming the fact of glycosylation of hemoglobin, which lowers oxygen-carrying capacity, that promotes hypoxia [26]. Barman et al. [12, 17] showed by using SERS that a high level of glucose in the blood not only influences protein function but also changes the structure of the heme. Importantly, the presence of subtle but distinct features in the difference spectra between Hb and HbA1c deposits highlights the sensitivity of the proposed approach to very small structural variations in the protein molecules. The variations in the two protein spectra can then be attributed to structural changes in hemoglobin molecules related to the binding of a glucose moiety [17, 27, 28]. For pyrrole rings scattering bands of δ(pyr deform)$_{sym}$, ν(pyr breathing), ν(pyr half-ring)$_{sym}$ at 689/692, 750/733, 1339/1345 have been detected, respectively. The fact of increased bands intensity (from 5.15% for δ(pyr deform)$_{sym}$ to 19.9% for ν(pyr breathing)) in HbA1c has been assigned to pyrrole ring polarization changes. Shifts in the pyrrole ring band can be also assigned to the chemical bond length of pyrrole molecules inside the pyrrole complex and its outer bonds. According to Ref. [38], pyrrole complex can change it orientation inside the molecule. Based on theoretical results in Ref. [39] hemoglobin exists in an ordered arrangement, such that the heme-porphyrin planes are preferentially orientated parallel to the RBCs' equatorial plane. The glycation of red blood cells can be precisely estimated using the electric/dielectric losses and polarization changes, described in detail in Ref. [40]. These factors lead to the spectral differences between the detected spectral shifts in pyrrole complex. Blue shift in tryptophan (Trp) scattering band with lowered intensity (of 7.86%) has been detected for Hb1A1c at 871 cm^{-1}. A slight blue shift in protein skeletal vibration and glutathione bands, substantially increased by 17.5% in the HbA1c case has been detected and this fact could be a possible marker of protein glycosylation [29]. No intensity changes have been detected in strong blue-shifted ν(C$_a$,C$_m$)$_{asym}$ band at 1596 cm^{-1} and 1580 cm^{-1} for Hb and HbA1c, respectively. The 16 cm^{-1} spectral shift can be explained by a change in the microenvironment of phenylalanine as a result of the transition of the molecule to the glycated form. The data for all well-defined positions of the maxima for Hb and HbA1c are given in Table 1.

Table 1 Well-defined Raman peak positions of Hb and HbA1c (cm^{-1}) and tentative assignments in "fingerprint" region*.

Hb	HbA1c	Vibrational modes	Reference	Δ_{int},%
689 vw	692 wsh	δ(pyr deform)$_{sym}$	[30]	5.15
750 vwsh	733 w	ν(pyr breathing), Trp	[11]	19.9
876 wv	871 wv	Trp	[16]	–7.86
976 mbr	980 mbr	p:Skeletal vibration, Glu	[11]	17.5
1136 wbr	1141 vwbr	δ(=C$_b$H$_2$)$_4$	[31]	5.33
1243 s	1248 s	δ(C$_m$H)	[27]	7.97
1339 m	1345 vwsh	ν(pyr half-ring)$_{sym}$, δ(C-C-H)	[16, 32]	12.52
1596 vs	1580 vs	ν(C$_a$,C$_m$)$_{asym}$, Phe	[11]	0
2933 s	2934 s	ν(CH$_3$)	[33]	10.03
3510 wbr	3512 mbr	H$_2$O	[30]	–54.85

*Abbreviations: w – weak; vw – very weak; m – medium; s – strong; vs – very strong; sh – shoulder; br – broad; δ – deformation vibration; ν – stretching vibration; Trp – tryptophan; Glu – glutathione; p – protein; Phe – phenilalnine;

$$\Delta_{\text{int}} = \frac{I_{Hb} - I_{HbA1c}}{I_{Hb}} \times 100.$$

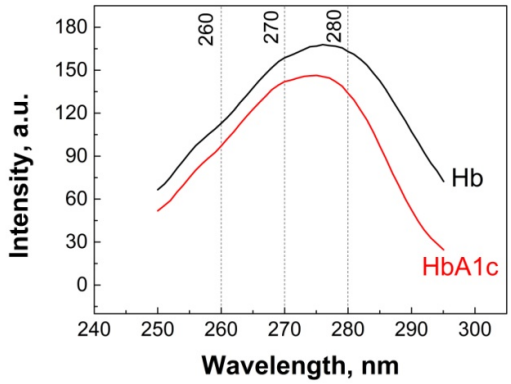

Fig. 3 Fluorescence excitation spectra of Hb and HbA1c.

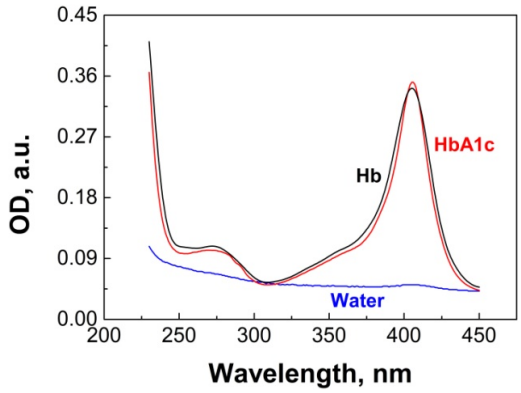

Fig. 4 Spectra of optical density of Hb, HbA1c and water.

The wavelengths of 260, 270, and 280 nm excitation of the fluorescence spectrum were selected for fluorescent analysis. The fluorescence excitation spectrum and spectrum of optical density of HbA1c and water for the selected region of excitation wavelengths are shown in Figs. 3, 4. These excitation wavelengths were chosen because of the published data where the peak of the hemoglobin fluorescence spectrum observed at 320 nm corresponds to the fluorescence of tryptophan that absorbs UV radiation with maxima at 220 nm and 280 nm and fluoresces in proteins at 328 ÷ 350 nm [20, 21]. Fig. 5 shows fluorescence spectra of solutions of Hb and HbA1c at excitation wavelengths of 260, 270, and 280 nm. The obtained spectral dependences were processed by Gaussian analysis in the program OriginLab Pro. The main parameters of fluorescence spectra of hemoglobin and glycated hemoglobin are given in Table 2.

According to the analysis of SERS spectra the vibrational activity of the constituent of the protein part of hemoglobin changes in the molecule HbA1c, while the detected fluorescence can be a fluorescence of the tryptophan and tyrosine parts of the molecule. The shift in the position of the peak in the short-wavelength region of the fluorescence spectrum of HbA1c for different excitation wavelengths can be explained by an increase in the contribution of tyrosine fluorescence. The change in the position of the fluorescence maximum of hemoglobin for different excitation wavelengths is explained by the change of the contribution of fluorescence of tryptophan and tyrosine. The amplification of the oscillations of tryptophan leads to quenching of tyrosine emission.

Analysis of SERS and fluorescence spectra showed that for the HbA1c molecule a partial quenching of tryptophan fluorescence occurs caused by increased vibrations of molecule nearby tryptophan, as a result, the contribution of tyrosine fluorescence increases. The relative change in fluorescence intensity of tryptophan and tyrosine leads to the formation of composite spectra, the position of the maxima of which is different from Hb.

For the first time in this paper, we have studied HbA1c dispersion and RI temperature increments in a wide spectral range using Abbe prism refractometry. Fig. 6a shows the dispersion of the RI of glycated and non-glycated hemoglobin solutions at 25 °C. The RI was measured for a temperature range of 23–43 °C for three selected wavelengths, 546, 589, 644, and 930 nm. The temperature dependence of the RI is shown in Fig. 6b.

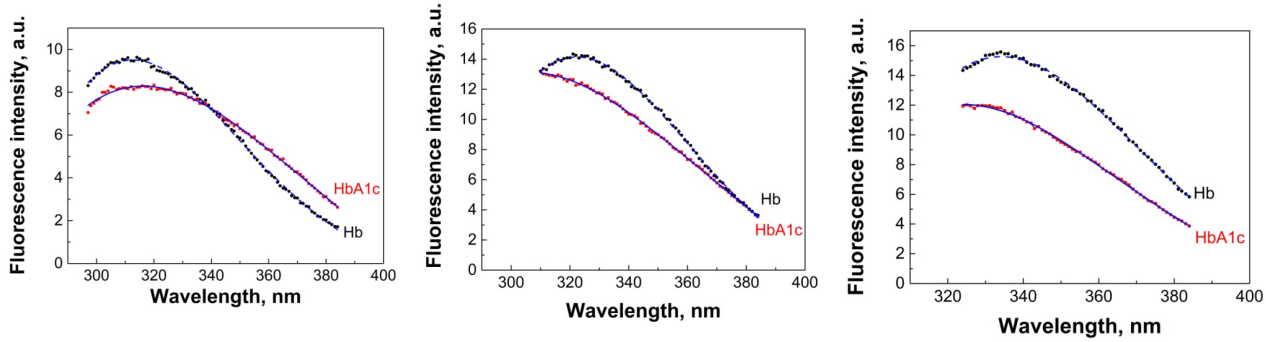

(a) (b) (c)

Fig. 5 Fluorescence spectra of Hb and HbA1c solutions with optical density of 0.1 at excitation wavelengths: (a) 260 nm; (b) 270 nm; (c) 280 nm (Hb– ■ (Black squares), HbA1c– ●(Red circles), Gaussian analysis – Blue lines).

Table 2 Parameters of fluorescence spectra of Hb and HbA1c: FWHM is the full width on half-maximum, FI is the fluorescence intensity (a.u.), and R^2 is the correlation coefficient.

Excitation wavelength	260 nm				270 nm				280 nm			
	λ, nm	FWHM	FI, a.u.	R^2	λ, nm	FWHM	FI, a.u.	R^2	λ, nm	FWHM	FI, a.u.	R^2
Hb	312	86	9.44	0.998	322	87	13.98	0.999	334	82	15.22	0.999
HbA1c	317	112	8.24	0.999	303	145	13.08	0.999	322	98	12.23	0.998
$\Delta_{HbA1c-Hb}$	5	26	0.35	–	–19	58	2.6	–	–12	16	–2.35	–

Table 3 Refractive index for $T = 0$ °C(n_0) and temperature increment (dn/dT) from the Eq. (1).

	546 nm		589 nm		644 nm		930 nm	
	n_0	$-dn/dT$, $\times10^{-4}$ °C^{-1}	n_0	$-dn/dT$, $\times10^{-4}$ °C^{-1}	n_0	$-dn/dT$, $\times10^{-4}$ °C^{-1}	n_0	$-dn/dT$, $\times10^{-4}$ °C^{-1}
Hb	1.3389 (±0.0005)	1.08 (±0.16)	1.3374 (±0.0003)	1.05 (±0.09)	1.3356 (±0.0004)	0.98 (±0.10)	1.3306 (±0.0003)	0.96 (±0.12)
HbA1c	1.3401 (±0.0005)	1.44 (±0.11)	1.3384 (±0.0003)	1.38 (±0.10)	1.3364 (±0.0003)	1.30 (±0.10)	1.3314 (±0.0003)	1.29 (±0.13)
$\Delta_{HbA1c-Hb}$	0.0012	0.36	0.0010	0.33	0.0008	0.32	0.0008	0.33

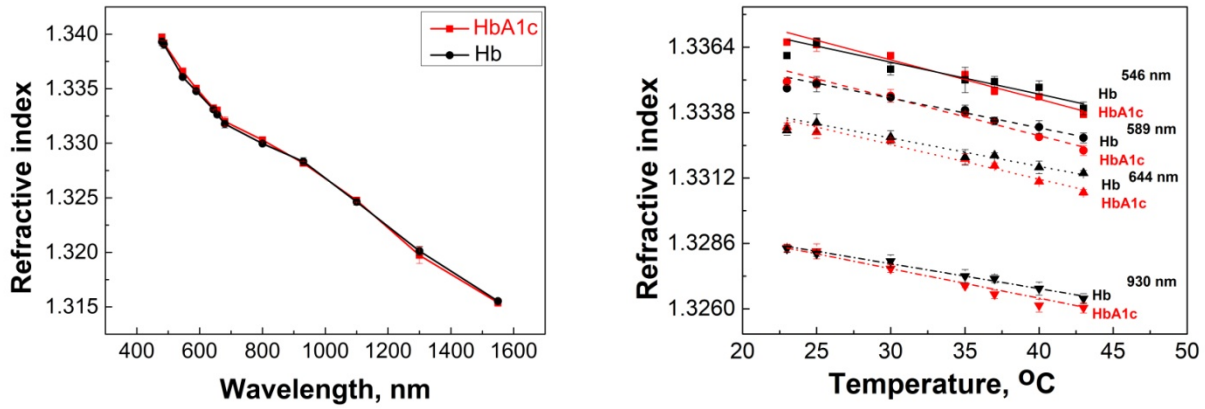

(a) (b)

Fig. 6 Dispersion measured at 25 °C (a) and temperature (b) dependencies of RI of Hb and HbA1c solutions at a concentration of 3 g/l.

The temperature dependence for the interval 23–43 °C was approximated by a linear function:

$$n(T) = n_0 + (dn/dT)T, \quad (1)$$

where n_0 is the RI for $T = 0$ °C; dn/dT is the RI derivative with respect to temperature or the temperature increment of the RI. The estimated values of n_0 and dn/dT for glycated and non-glycated hemoglobin forms are given in Table 3.

Based on the results obtained, we found an increase of the modulus of temperature increment for the glycated form of hemoglobin by an average of $(0.34 \pm 0.02)\times10^{-4}$ °C^{-1} for the wavelengths 546, 589, 644, and 930 nm. The total derivative of the RI with respect to temperature is related to the effect of thermal expansion and the temperature dependence of the molecular polarizability [34, 35]. In connection with this, the differences obtained in this study for Hb and HbA1c can be explained by their different molecular structure. The relationship between the polarizability of a molecule and the RI of a medium composed of these molecules is well described [34, 35]. The additivity rule is valid for molecular complexes consisting of molecules with different polarizabilities. In this case, the total polarizability is considered equal to the sum of the polarizability of each of the molecules. Thus, the molecular complex of hemoglobin with glucose has a larger molecular polarizability and RI depends on the content of charged amino acids in the molecule. The

dependence of the RI of dry erythrocytes from diabetic patients on pH (pH = 2–13) and, consequently, on the charge of the protein R-group was shown by Mazarevica et al. by using polarization-sensitive interference microscopy for the wavelength 550 nm [36].

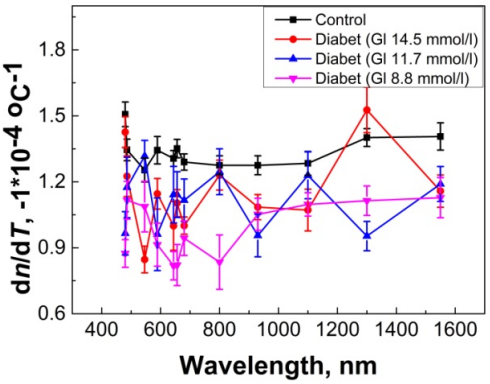

(a)

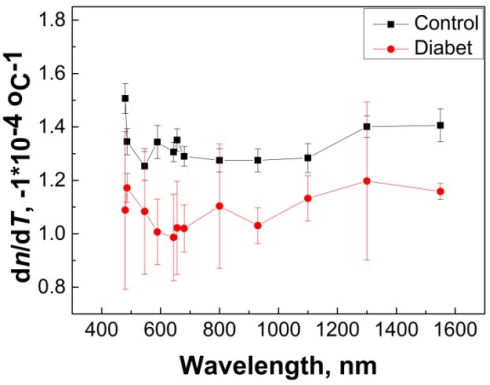

(b)

Fig. 7 The wavelength dependence of RI temperature increment: (a) for healthy volunteers and diabetic patients with different levels of free glucose; (b) mean values for healthy (control) and diabetic groups.

We also studied the temperature dependence of the RI of hemoglobin obtained from whole blood of healthy people (control group) and patients with diabetes mellitus (diabetic group). In order to avoid influence of variations of hemoglobin concentration from sample to sample, the normalization of RI values for different patients was carried out by using this formula:

$$n_{\text{norm}} = \frac{n_\lambda}{n_{\lambda,\max}}, \qquad (2)$$

Figs. 7a and 7b show that for the diabetic group the temperature increment is lower than for the healthy (control) group. It should be noted that in these samples a hemoglobin solution consisting of various hemoglobin fractions was studied, the concentration of which considerably exceeds the physiological concentration of glycated hemoglobin. However, the graphs show that for the diabetic group the temperature increment is lower than for the healthy (control) group which is contradictory to data obtained for the temperature increment of glycated and non-glycated hemoglobin samples prepared from hemolysate of HbA1c and lyophilized powder of human Hb, respectively. Evidently, this is due to differences in the studied samples. Dry for Hb / HbA1c measurements and Hemoglobin extracted from the whole blood of healthy and diabetic subjects may contain additional molecular components that may have different temperature increments. The high level of free glucose in the blood (8.8–14.5 mmol/l) also may have an impact on the value of increment. In fact, statistically significant differences of measured RI temperature increments of hemoglobin from healthy and diabetic subjects on the wavelengths 589, 644, 656, 680, 930, 1100, and 1500 nm are found.

Thus, optical methods used in the work demonstrate the possibility of detection of small amounts of HbA1c on the background of Hb in their mixtures directly without any chemical reaction. High sensitivity has the refractometric method applied for the first time to measure RI temperature increments for different wavelengths.

4 Conclusion

Analysis of three different optical methods revealed the presence of characteristic features allowing for discrimination glycated HbA1c and normal Hb hemoglobins. SERS demonstrated well detectable differences of Raman bands and their intensities mainly in the “fingerprint” region of 500–1800 cm^{-1}. Revealed features can be used as HbA1c markers in hemoglobin mixtures. Fluorescence spectroscopy showed the presence of characteristic distinctive features for glycated hemoglobin at excitation on the wavelength of 270 nm. The average increase in the refractive index temperature increment modulus of HbA1c in comparison to Hb in the visible and NIR spectral regions is of $(0.34 \pm 0.02)\times10^{-4}\,°C^{-1}$.

The data obtained in this work confirm and supplement those that are available in the literature, and can also serve as a basis for further study of the optical properties of glycated hemoglobin and other glycated proteins. Data received are important for the development of optical diagnostic and therapeutic methods, in particular for *in vivo* fluorescent and photoacoustic cytometry of melanoma cells in the bloodstream of diabetic patients.

Disclosures

The authors have no relevant financial interests in this article and no potential conflicts of interest to disclose.

Acknowledgements

I. G. Samusev and A. Y. Zyubin was supported by state contract of the RF Ministry of Science and Higher Education of the Russian Federation (FZWM-2020-0003).

E. N. Lazareva acknowledges financial support of the RFBR grant 20-32-90058 for fluorescence and refraction measurements.

A. B. Bucharskaya and V. V. Tuchin acknowledge financial support of the grant under the Decree of the Government of the Russian Federation No. 220 of 09 April 2010 (Agreement No. 075-15-2021-615 of 04 June 2021).

References

1. M. Smiga, J. W. Smalley, P. Ślęzak, J. L. Brown, K. Siemińska, R. E. Jenkins, E. A. Yates, and T. Olczak, "Glycation of Host Proteins Increases Pathogenic Potential of Porphyromonas gingivalis," International Journal of Molecular Sciences 22(12), 12084 (2021).
2. S. Yazdanpanah, M. Rabiee, M. Tahriri, M. Abdolrahim, A. Rajab, H. E. Jazayeri, and L. Tayebi, "Evaluation of glycated albumin (GA) and GA/HbA1c ratio for diagnosis of diabetes and glycemic control: A comprehensive review," Journal Critical Reviews in Clinical Laboratory Sciences 54(4), 3 (2017).
3. E. Selvin, M. W. Steffes, H. Zhu, K. Matsushita, L. Wagenknecht, J. Pankow, J. Coresh, and F. L. Brancati, "Glycated hemoglobin, diabetes, and cardiovascular risk in nondiabetic adults," New England Journal of Medicine 362(9), 800–811 (2010).
4. T. Pan, M. Li, J. Chen, and H. Xue, "Quantification of glycated hemoglobin indicator HbA1c through near-infrared spectroscopy," Journal of Innovative Optical Health Sciences 7(4), 1350060 (2014).
5. P. Dong, H. Lin, K. Huang, and J. Cheng, "Label-free quantitation of glycated hemoglobin in single red blood cells by transient absorption microscopy and phasor analysis," Science Advances 5(5), eaav0561 (2019).
6. Executive Summary: Standards of Medical Care in Diabetes, Diabetes Care 33 (Supplement 1), S4-S10 (2010).
7. V. V. Tuchin, A. Tárnok, and V. P. Zharov, "In vivo flow cytometry: A horizon of opportunities," Cytometry Part A 79(10), 737–745 (2011).
8. D. A. Nedosekin, M. A. Juratli, M. Sarimollaoglu, C. L. Moore, N. J. Rusch, M. S. Smeltzer, V. P. Zharov, and E. I. Galanzha, "Photoacoustic and photothermal detection of circulating tumor cells, bacteria and nanoparticles in cerebrospinal fluid in vivo and ex vivo," Journal of Biophotonics 6(6–7), 523–533 (2013).
9. D. A. Nedosekin, M. Sarimollaoglu, J.-H. Ye, E. I. Galanzha, and V. P. Zharov, "In vivo ultra-fast photoacoustic flow cytometry of circulating human melanoma cells using near-infrared high-pulse rate lasers," Cytometry Part A 79(10), 825–833 (2011).
10. J. Q. Lin, R. Chen, S. Feng, J. Pan, Y. Li, G. Chen, M. Cheng, Z. Huang, Y. Yu, and H. Zeng, "A novel blood plasma analysis technique combining membrane electrophoresis with silver nanoparticle based SERS spectroscopy for potential applications in non-invasive cancer detection," Nanomedicine: Nanotechnology, Biology and Medicine 7(5), 655–663 (2011).
11. J. Lin, J. Lin, Z. Huang, P. Lu, J. Wang, X. Wang, and R. Chen, "Raman spectroscopy of human hemoglobin for diabetes detection," Journal of Innovative Optical Health Sciences 7(1),1350051 (2014).
12. I. Barman, N. C. Dingari, J. W. Kang, G. L. Horowitz, R. R. Dasari, and M. S. Feld, "Raman spectroscopy-based sensitive and specific detection of glycated hemoglobin," Analytical Chemistry 84(5), 2474−2482 (2012).
13. O. S. Zhernovaya, V. V. Tuchin, and I. V. Meglinski, "Monitoring of blood proteins glycation by refractive index and spectral measurements," Laser Physics Letters 5(6), 460–464 (2008).
14. E. Shirshin, O. P. Cherkasova, T. Tikhonova, E. Berlovskaya, A. V. Priezzhev, and V. Fadeev, "Native fluorescence spectroscopy of blood plasma of rats with experimental diabetes: identifying fingerprints of glucose-related metabolic pathways," Journal of Biomedical Optics 20(5), 051033 (2015)
15. S. Y. Feng, R. Chen, J. Lin, J. Pan, G. Chen, Y. Li, M. Cheng, Z. Huang, J. Chen, and H. Zeng, "Nasopharyngeal cancer detection based on blood plasma surface-enhanced Raman spectroscopy and multivariate analysis," Biosensors and Bioelectronics 25(11), 2414–2419 (2010).
16. H. W. Han, X. L. Yan, R. X. Dong, G. Ban, and K. Li, "Analysis of serum from type II diabetes mellitus and diabetic complication using surface-enhanced Raman spectra (SERS)," Applied Physics B 94(4), 667– 672 (2009).
17. I. Barman, N. C. Dingari, J. W. Kang, G. L. Horowitz, R. R. Dasari, and M. S. Feld, "Raman spectroscopy based sensitive and specific detection of glycated hemoglobin," Analytical Chemistry 84(5), 2474–2482 (2012).
18. M. S. Kiran, T. Itoh, K.-I. Yoshida, N. Kawashima, V. Biju, and M. Ishikawa, "Selective Detection of HbA1c Using Surface Enhanced Resonance Raman Spectroscopy," Analytical Chemistry 82(2), 1342−1348 (2010).
19. M. Sackmann, S. Bom, T. Balster, and A. Materny, "Nanostructured gold surfaces as reproducible substrates for surface-enhanced Raman spectroscopy," Journal of Raman Spectroscopy 38(3), 277−282 (2007).
20. J. T. Liu, L.-Y. Chen, M.-C. Shih, Y. Chang, and W.-Y. Chen, "The investigation of recognition interaction between phenyl boronate monolayer and glycated hemoglobin using surface plasmon resonance," Analytical Biochemistry 375(1), 90–96 (2008).
21. J. Li, K.-W. Chang, C.-H. Wang, C.-H. Yang, S.-C. Shiesh, and G.-B. Lee, "On-chip, aptamer-based sandwich assay for detection of glycated hemoglobins via magnetic beads," Biosensors and Bioelectronics 79, 887–893 (2016).

22. P. Giannios, S. Koutsoumpos, K. G. Toutouzas, M. Matiatou, G. C. Zografos, and K. Moutzouris, "Complex refractive index of normal and malignant human colorectal tissue in the visible and near-infrared," Journal of Biophotonics 10(2), 303–310 (2017).
23. S. Carvalho, N. Gueiral, E. Nogueira, R. Henrique, L. Oliveira, and V. V. Tuchin, "Wavelength dependence of the refractive index of human colorectal tissues: comparison between healthy mucosa and cancer," Journal of Biomedical Photonics and Engineering 2(4), 040307 (2016).
24. K. Zirk, H. Poetzschke, "On the suitability of refractometry for the analysis of glucose in blood-derived fluids," Medical Engineering & Physics 26(6), 473–481 (2004).
25. K. Zirk, H. Poetzschke, "A refractometry-based glucose analysis of body fluids," Medical Engineering & Physics 29(4), 449–458 (2007).
26. S. I. Sherwani, H. A. Khan, A. Ekhzaimy, A. Masood, and M. K. Sakharkar,"Significance of HbA1c test in diagnosis and prognosis of diabetic patients," Biomarker Insights 11, BMI-S38440 (2016).
27. B. R. Wood, P. Caspers, G. J. Puppels, S. Pandiancherri, and D. McNaughton,"Resonance Raman spectroscopy of red blood cells using near-infrared laser excitation," Analytical and Bioanalytical Chemistry 387(5), 1691–1703 (2007).
28. R. Ghosh Moulick, J. Bhattacharya, S. Roy, S. Basak, and A. K. Dasgupta, "Compensatory secondary structure alterations in protein glycation," Biochimica et Biophysica Acta (BBA) – Proteins and Proteomics 1774, 233−242 (2007).
29. D. P. Cowcher, T. Deckert-Gaudig, V. L. Brewster, L. Ashton, V. Deckert, and R. Goodacr, "Detection of protein glycosylation using tip-enhanced Raman scattering," Analytical Chemistry 88(4), 2105–2112 (2016).
30. Q. Sun, "The Raman OH stretching bands of liquid water," Vibrational Spectroscopy 51(2), 213–217 (2009).
31. G. Rusciano, A. C. De Luca, G. Pesce, and A. Sasso, "Raman tweezers as a diagnostic tool of hemoglobin-related blood disorders," Sensors 8(12), 7818–7832 (2008).
32. C. R. Yonzon, C. L. Haynes, X. Zhang, J. T. Walsh, and R. P. Van Duyne, "A glucose biosensor based on surface-enhanced Raman scattering: improved partition layer, temporal stability, reversibility, and resistance to serum protein interference," Analytical Chemistry 76(1), 78–85 (2004).
33. J. Lin, Y. Zeng, J. Lin, J. Wang, L. Li, Z. Huang, B. Li, H. Zeng, and R. Chen, "Erythrocyte membrane analysis for type II diabetes detection using Raman spectroscopy in high-wavenumber region," Applied Physics Letters 104(10), 104102 (2014).
34. A. I. Erokhin, N. V. Morachevskii, and F. S. Faizullov, "Temperature dependence of the refractive index in condensed media," Journal of Experimental and Theoretical Physics 74, 1336–1341 (1978).
35. M. V. Volkenshtein, Molecular Optics, Gosteskhizdat, Moscow (1951) [in Russian].
36. G. Mazarevica, T. Freivalds, and A. Jurka, "Properties of erythrocyte light refraction in diabetic patients," Journal of Biomedical Optics 7(2), 244–247 (2002).
37. T. K. Das, M. Couture, Y. Ouellet, M. Guertin, and D. L. Rousseau, "Simultaneous observation of the O-O and Fe-O_2 stretching modes in oxyhemoglobins," Proceedings of the National Academy of Sciences 98(2), 479–484 (2001).
38. C. G. Atkins, K. Buckley, M. W. Blades, and R. F. B. Turner, "Raman spectroscopy of blood and blood components," Applied Spectroscopy 71(5), 767–793 (2017).
39. S. Ahlawat, A. Chowdhury, N. Kumar, A. Uppal, R. S. Verma, and P. K. Gupta, "Polarized Raman Spectroscopic Investigations on Hemoglobin Ordering in Red Blood Cells," Journal of Biomedical Optics 19(8), 87002 (2014).
40. S. Abdalla, F. Farsaci, E. Tellone, W. Shirbeeny, A. M. Hassan, F. Bahabri, and S. Kandil, "Hemoglobin glycation increases the electric charges on red blood cells: Effects of dielectric polarization," Materials Chemistry and Physics 276, 125348 (2022).